Available online at www.sciencedirect.com

ScienceDirect

Procedia Structural Integrity 24 (2019) 625–635

Structural Integrity Procedia

www.elsevier.com/locate/procedia

AIAS 2019 International Conference on Stress Analysis

A simplified multiscale model of degenerate graphite clusters in grey cast iron

Matteo Cova[a], Paolo Livieri[b], Raffaella Rizzoni[b]*, Roberto Tovo[b]

[a]*Sacmi Imola S. C., Via Selice, 17, 40026 Imola (Bologna) Italy*
[b]*Department of Engineering, University of Ferrara, Via Saragat 1, 44122 Ferrara, Italy*

Abstract

To take into account the weakening effect of defects clusters in real microstructures, we propose a multiscale model in a two-dimensional setting. At a small scale, single defects are described as elliptical voids randomly distributed and randomly oriented in an isotropic matrix. Using an effective field method proposed by Tandon and Weng [5,6], the effective properties of a porous equivalent material can be estimated in a simple closed form. At a larger scale, defects clusters are modelled as single large elliptical inclusions characterized by the weakened effective properties calculated in the first step and embedded in an infinite, elastic, isotropic matrix under remote loading. The method allows to examine the dependence of defects interaction on some basic microstructure parameters (porosity density, voids aspect ratio, inclusion aspect ratio).

Keywords: Defects cluster; effective elastic moduli; stress concentration factor.

1. Introduction

Defects morphology largely affects the mechanical and strength properties of grey cast iron, cf. Hütter et al. (2015), Rausch et al. (2010). Irregularly shaped graphite clusters can be sites of stress concentrations and crack initiations, and fatigue properties are well known to correlate to microstructural parameters, like graphite inclusions shape, size and

* Corresponding author. Tel.: +0-39-0532-974959; fax: +0-000-000-0000 .
E-mail address: raffaella.rizzoni@unife.it

10.1016/j.prostr.2020.02.055

spacing between them, cf. Costa et al (2010), and Mottitschka et al. (2012). Due to the complex defects' distribution and shape, a numerical estimate of the exact interaction between these complex morphologies can be very difficult, even in a linear elastic framework. In cast iron, like in most part of natural materials, defects and voids come in a mixture of diverse shapes, as shown in Fig. 1a. A possible simplifying assumption is to replace them by elliptical holes of different shapes and aspect ratios, whose distribution could be identified from microstructural information, as done in Fig. 1a.

In a previous paper (see Cova et al. 2017) the iteration between two ellipses in a plate under tensile loading was considered, whereas in this contribution we report on some ongoing work based on a novel simplified multiscale approach in a 2D setting (plane strain). The modeling strategy is based on two consecutive steps. The first step focuses on a small scale, where the complex microstructure internal to degenerate graphite clusters is modeled as a random distribution of randomly-oriented elliptical voids (the defects) in an isotropic matrix, see Fig. 1b.

Using an effective field method firstly proposed by Weng (1984) and further developed by Tandon and Weng (1984, 1986) and Zhao and Weng (1990), the effective elastic properties of a porous equivalent material can be estimated in a simple closed analytical, albeit approximated form, depending only on the matrix elastic parameters, the voids aspect ratio and the porosity density. In Section 2, we report the analytical expressions of the effective Young's modulus and Poisson ratio for a two-dimensional elastic plate weakened by a family of equal elliptical voids randomly oriented inside an elementary cell. The expressions have been validated via a FE analysis and a good agreement has been found.

The second step considers a larger scale, where a defect cluster is modeled as single elliptical inclusion embedded in an isotropic matrix and characterized by the weakened effective elastic properties calculated at the previous level, see Fig. 1c. Eshelby's fundamental solution (1957, 1959, 1961) allows to analyze the dependence of the stress state, internal and external to the inclusion (the defects cluster), on some basic microstructure parameters (voids aspect ratio, porosity density, and inclusion aspect ratio). Our analysis performed in Section 3 focuses on the stress peaks at the interface between the inclusion and the matrix and on their dependence on the microstructure parameters.

The model presented in this paper is simplified, in view of the many adopted approximations. Firstly, the model is two-dimensional, while a three-dimensional setting would be more appropriate, especially with the modern available techniques of high resolution tomographic imaging. Next, a family of equal ellipses has been considered. Weng's approach is however enough general to take into account several families of different elliptical voids. Inhomogeneities found in real microstructures are usually non-ellipsoidal, so replacing a non-elliptical inclusion with an elliptical one is clearly a major simplifying assumption. Like in many other various micromechanical schemes available in the literature, cf. Shen and Yi (2001) and Feng et a. (2003), our choice of elliptical defects is related to the special feature of Eshelby's fundamental solution, that the stress-strain field inside an elliptical inclusion in an infinite plate is uniform. Zou et al. (2010) and Zou (2011) have discussed the limit of applications of Eshelby's fundamental solution, and have concluded that the elliptical approximation over a convex inclusion induces a small relative error and can be considered as valid. Finally, other simplifications in our model derive from the choice of the size (and shape) of the inclusion modeling the defects cluster, which we do not discuss here and postpone to future work. Other possible developments of the present approach could focus on the interaction of a single defects cluster with a free boundary or with other defects clusters.

Taking into account all the discussed approximations, the results presented in the present paper can be considered as a first step towards a more general analysis.

The approach presented in this paper may appear to be similar to the models proposed by Shen and Yi (2001) and Feng et a. (2003), but it is indeed different for the following reasons. The model proposed by Shen and Yi (2001) focuses on calculating the effective elastic moduli of a heterogeneous material, while our final goal is the analysis of the stress peaks and their dependence on the microstructure parameters. Feng et al. (2003) present a novel method to take into account the microcracks interaction. In their analysis, they apply Kachanov's method to calculate the effective elastic moduli of microcracked materials, while we follow the approach proposed by Weng (1984) and Tandon and Weng (1984, 1986).

Nomenclature

C_{eff}	effective elastic tensor
C	matrix elastic tensor
λ	voids volume fraction or porosity density
e^0	average strain in the matrix
$\langle e^* \rangle$	average strain over all orientations
I	unit fourth order tensor
S	Eshelby's tensor
$Q(\theta)$	transformation tensor
θ	void orientation angle
a,b	ellipse semi-axes
E,ν	Young's modulus and Poisson ratio of the matrix
E_{eff},ν_{eff}	Young's modulus and Poisson ratio of porous material from Weng's model
χ	voids aspect ratio
E_{mix}, ν_{mix}	Young's modulus and Poisson ratio of porous material from mixture rule
ψ	inclusion orientation angle
t	inclusion aspect ratio

2. Effective elastic moduli of a porous plate

At the lowest level of the multiscale model, the weakening effect induced by the presence of graphite inclusions is modeled using the micromechanical approach proposed by Weng (1984) and further developed by Tandon and Weng (1984, 1986), and by Zhao and Weng (1990). The approach considers a composite made of ellipsoidal inclusions, aligned or randomly-oriented, and homogeneously dispersed in an elastic matrix with different elastic properties. Mori and Tanaka's (1973) concept of "average stress" in the matrix and Eshelby's fundamental solution (1957, 1959, 1961) are combined to obtain the effective elastic moduli of the composite. Though approximated, the approach leads to the exact solution for the effective bulk modulus of an isotropic composite calculated by Hill (1963) when the shear moduli of the inclusion and matrix material are equal, cf. Weng (1984).

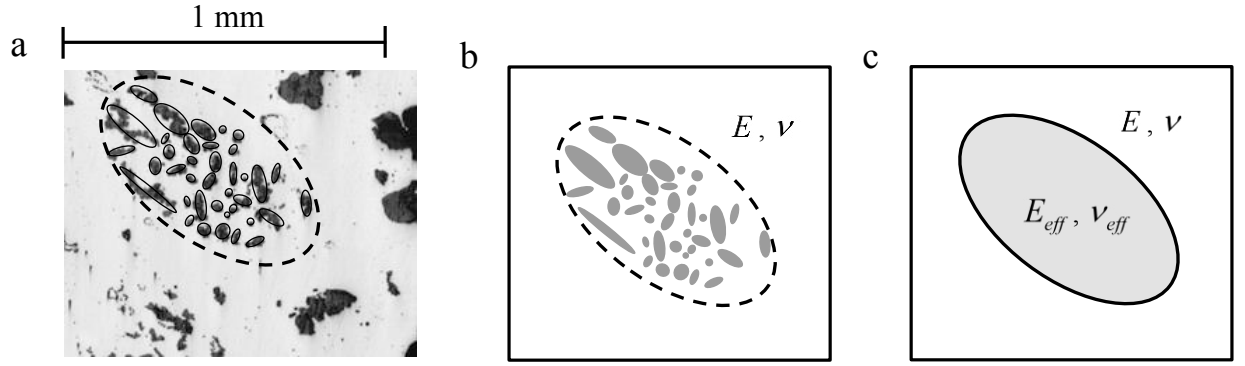

Fig. 1. Scheme of the simplified multiscale approach: (a) degenerate graphite cluster; (b) cluster model as a fictitious elliptic inclusion incorporating many elliptical holes (in gray); (c) final elliptic inclusion filled with equivalent weakened material (in light gray) and embedded in the original matrix.

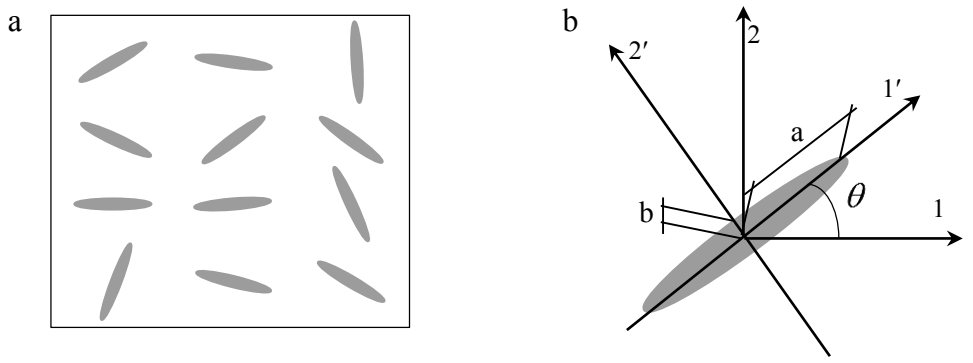

Fig. 2. (a) Schematic representation of a porous material obtained by homogeneously distributed, equal, randomly-oriented elliptical voids in an elastic matrix; (b) angle θ defining the orientation of the generic void.

For a composite with equal, elliptical, homogeneously dispersed, randomly-oriented voids, the effective elastic tensor C_{eff} solves the equation

$$C_{eff}(e^0 + \lambda\langle e^*\rangle) = Ce^0, \tag{1}$$

where C is the elastic tensor of the matrix, λ is the voids volume fraction, $e^0$is the average strain in the matrix in the composite system when there exists only a single inclusion, and $\langle e^*\rangle$ is the average of the equivalent transformation strains of the inclusions over all orientations. In a plane case, $\langle e^*\rangle$ can be expressed as follows:

$$\langle e^*\rangle = \frac{1}{\pi}\int_0^{\pi} Q^T(\theta)((I-S)^{-1}(Q(\theta)e^0Q^T(\theta)))\,Q(\theta)d\theta. \tag{2}$$

Here, $I$is the unit fourth order tensor, S is Eshelby's tensor, and $Q(\theta)$ is the transformation tensor between the local (primed) axes and the global (unprimed) ones shown in Fig. 2b, and given by

$$Q(\theta) = \begin{pmatrix} cos(\theta) & sin(\theta) & 0 \\ -sin(\theta) & cos(\theta) & 0 \\ 0 & 0 & 1 \end{pmatrix}, \tag{3}$$

where θ is the angle defining the orientation of voids, cf. Fig. 2b.
Assuming plane strain conditions, considering an isotropic elastic behavior for the matrix, with Young's modulus E and Poisson ratio ν, and substituting the components of the Eshelby's tensor S given by Zhao and Weng (1990) into Equations (1-3), we obtain the following closed-form solution for the (in-plane) effective elastic constants of the porous material:

$$E_{eff} = \frac{E(1-\lambda)\left\{1+\nu+\lambda\left[2-4\nu+\left(\chi+\frac{1}{\chi}\right)(1-\nu)^2\right]\right\}}{(1+\nu)\left\{1+\lambda\left[1+\chi+\frac{1}{\chi}-\nu\left(2+\chi+\frac{1}{\chi}\right)\right]\right\}^2}, \tag{4}$$

$$\nu_{eff} = \frac{\left\{\lambda+\nu-\lambda\nu\left(2+\chi+\frac{1}{\chi}\right)+\lambda\nu^2\left(\chi+\frac{1}{\chi}\right)\right\}}{\left\{1+\lambda\left[1+\chi+\frac{1}{\chi}-\nu\left(2+\chi+\frac{1}{\chi}\right)\right]\right\}}. \tag{5}$$

These constants take simple explicit forms as a function of the cross-sectional aspect ratio $\chi = b/a$ of the voids, of their volume fraction λ, or porosity density, and of the matrix elastic moduli E and ν. More generally, the micromechanical approach proposed by Weng (1984) can treat hard, soft, or void inclusions with two- (ellipse, circle) and three-dimensional shapes (prolate, spherical and oblate) in a unified fashion.
For the proposed multiscale model, families of ellipses with different aspect ratios could be considered, in order to

better describe the real microstructure, cf. Fig. 1b.
In order to investigate the range of validity of relations (4) and (5), a parametric FE analysis has been performed, analyzing a plate of 100x200 mm under plane strain conditions with random distributions of elliptical voids inside a square elementary cell 10x10 mm. For the voids aspect ratio, χ, the following values have been considered: 0.1, 0.2, 0.4, 0.5, 1. The elastic constants of the matrix have been taken equal to $E = 206$ GPa and $\nu = 0.3$. Several random distributions of voids have been generated, cf. Fig. 3, and very small variations of the corresponding elastic properties calculated numerically have been observed. The plots of the elastic properties, $E_{eff}/(1-{\nu_{eff}}^2)$ and ν_{eff} calculated via FE analysis are illustrated in Figures 4 and 5, respectively, where the comparisons with the prediction given by relations (4) and (5) are also shown. In Figures 4 and 5, the estimates given by the following rules of mixtures

$$E_{mix} = (1-\lambda)E/(1-\nu^2), \tag{6}$$

$$\nu_{mix} = (1-\lambda)\nu \tag{7}$$

are visualized with dotted lines.

Figures 4 and 5 indicate a good general agreement between Equations (4) and (5) and the FE results, with a maximum relative difference of 26% for the effective plain strain elastic modulus (maximum attained at $\lambda = 0.502$ and $\chi = 1$), and of 14% for the effective Poisson ratio (maximum attained at $\lambda = 0.283$ and $\chi = 1$). The rule of mixtures, cf. Equations (6) and (7), gives over-stiff results, with a maximum relative difference of 106% for the effective plain strain elastic modulus (maximum attained at $\lambda = 0.636$ and $\chi = 1$), and of 104% for the effective Poisson ratio (maximum attained at $\lambda = 0.06$ and $\chi = 0.1$).

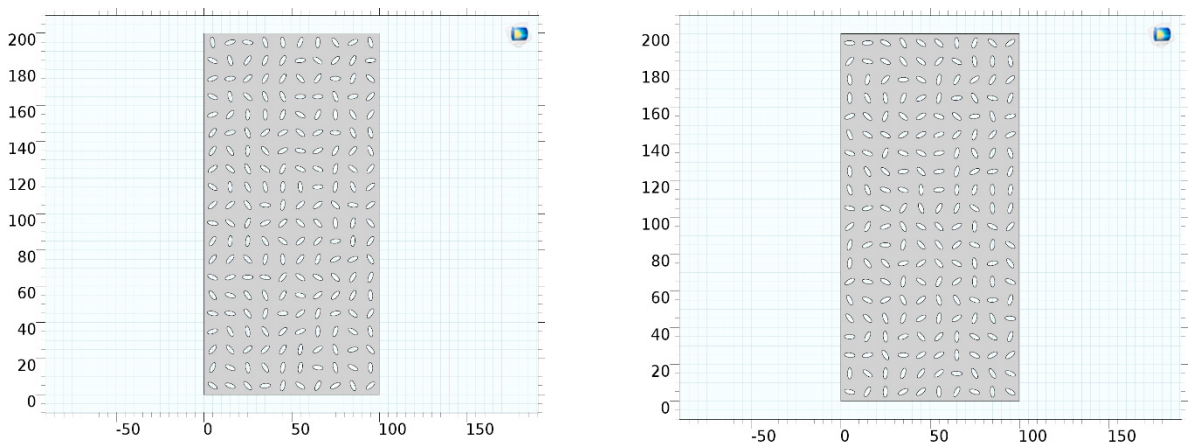

Fig. 3. Two reference geometries used in the FE analysis.

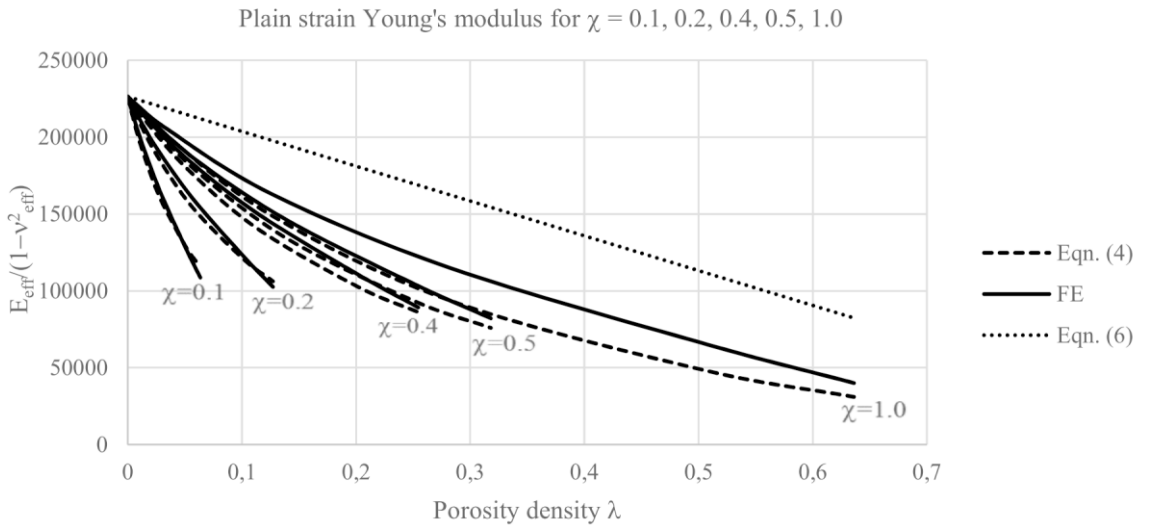

Fig. 4. Comparison between the effective plain strain elastic modulus $E_{eff}/(1-\nu_{eff}{}^2)$ numerically calculated via the FE analysis (continuous curves) and the prediction given by the approximated relation (4) (dashed curves). Different (continuous and dashed) curves refer to different voids aspect ratio χ. The prediction given by the rule of mixtures Eq. (6) is also shown (dotted line).

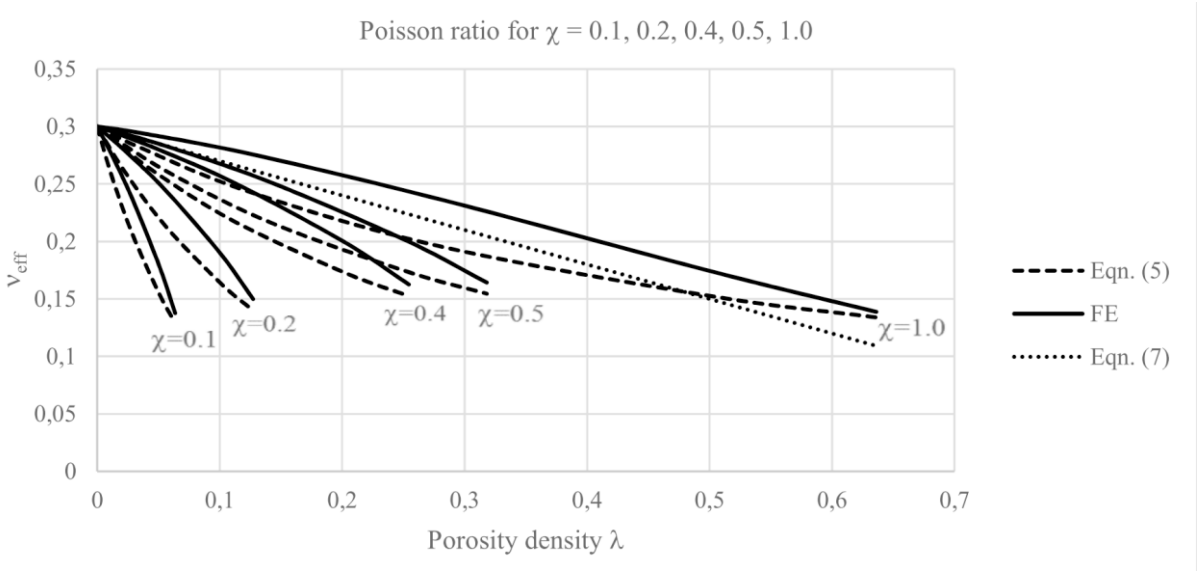

Fig. 5. Comparison between the effective Poisson ratio ν_{eff} numerically calculated via the FE analysis (continuous curves) and the prediction given by the approximated relation (5) (dashed curves). Different (continuous and dashed) curves refer to different voids aspect ratio χ. The prediction given by the rule of mixtures Eq. (7) is also shown (dotted line).

3. Stress intensity factors for inclusions weakened by porosity

In this Section, we analyze the stress state arising in the equivalent elliptic inclusion subject to unidirectional traction load applied at infinity, see Fig 6. In view of the elliptical shape, the uniformity of the stress-strain field in the inclusion allows to obtain an exact solution, firstly presented by Eshelby in a three-dimensional setting (1957, 1959, 1961).
Jin et al. (2014) have obtained the full field stress solution of Eshelby's problem in plane elasticity using the equivalent inclusion method. In this paper, the Equations (56) -(58) given by Jin et al. (2014) and providing the interior and exterior stress fields have been implemented in MATLAB® together with Equations (4) and (5) giving the weakened elastic moduli of the inclusion.
As a result, we have calculated the stress concentration factors (SCFs) at the matrix/inclusion interface, on the inclusion side and on the matrix side. For the matrix material, we have assumed $E = 206$ GPa and $\nu = 0.3$, as in Section 2.
The plots of the stress concentration factors shown in Fig. 7, 8 and 9 indicate their dependency on the porosity density λ, for inclusion orientation angles $\psi = 0, \frac{\pi}{6}, \frac{\pi}{4}$, respectively. In these Figures, the aspect ratio porosity has been chosen equal to $\chi = 0.1$, and the inclusion aspect ratio takes the values $t = 0.1, 0.5, 1, 2, 10$.
As the porosity density λ increases, the inclusion becomes softer, leading to relatively lower stress on the inclusion side and higher stress on the matrix side. Soft inclusions with the smallest aspect ratio $t = 0.1$ and lowest orientation angle ψ lead to the higher stress concentrations in the matrix.
Contour plots of the SCFs on the inclusion and matrix sides for voids' aspect ratio χ vs inclusion aspect ratio t at constant porosity density λ=0.25 and for the inclusion orientation angles of ψ=0, π/6, π/4 are shown in Fig. 10, 11 and 12.
Darkest points correspond to softest inclusions, leading to lower stress level on the inclusion side and higher stress concentrations on the matrix side. The plots reveal that higher stress concentrations (>4) occur for very small aspect ratios χ, t, or very small χ and large t, i.e. for voids and inclusion approaching a crack shape.

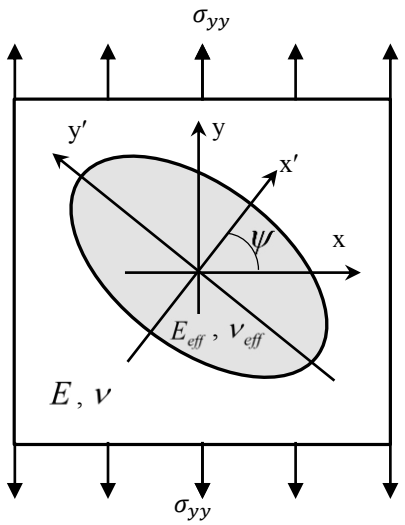

Fig. 6. Reference geometry and notation for the equivalent inclusion of Fig.1c subject to uniaxial traction at infinity.

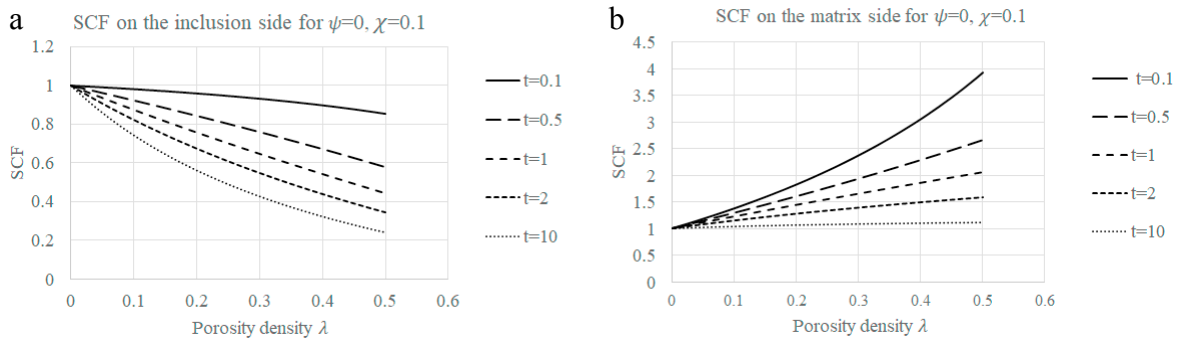

Fig. 7. Variation of the stress concentration factor on the inclusion side (a) and on the matrix side (b) with the porosity for inclusion orientation angle $\psi = 0$, aspect ratio porosity $\chi = 0.1$ and inclusion aspect ratios $t = 0.1, 0.5, 1, 2, 10$.

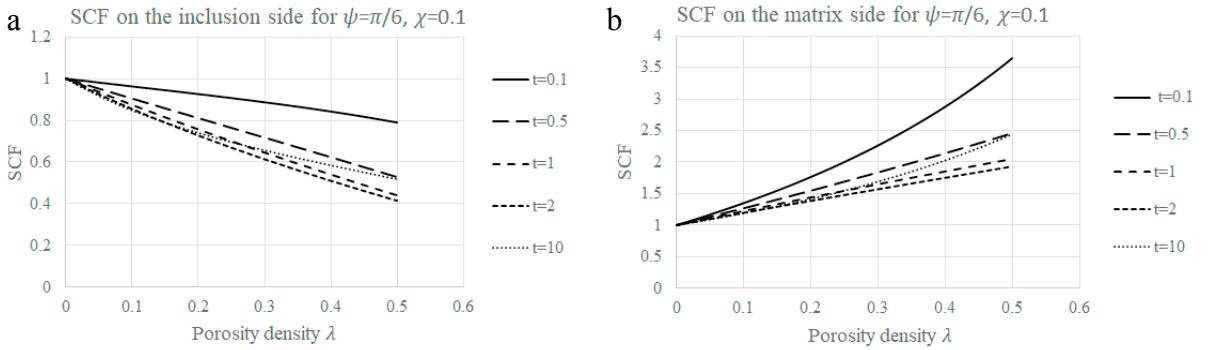

Fig. 8. Variation of the stress concentration factor on the inclusion side (a) and on the matrix side (b) with the porosity for inclusion orientation angle $\psi = \pi/6$, aspect ratio porosity $\chi = 0.1$ and inclusion aspect ratios $t = 0.1, 0.5, 1, 2, 10$.

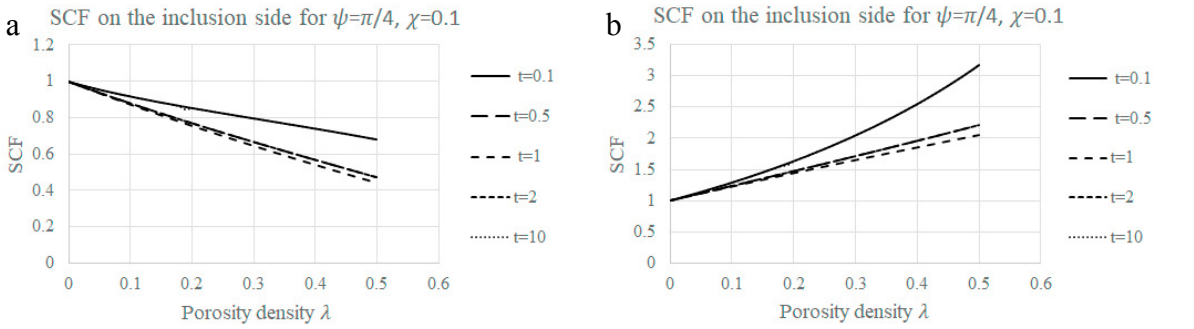

Fig. 9. Variation of the stress concentration factor on the inclusion side (a) and on the matrix side (b) with the porosity for inclusion orientation angle $\psi = \pi/4$, aspect ratio porosity $\chi = 0.1$ and inclusion aspect ratios $t = 0.1, 0.5, 1, 2, 10$.

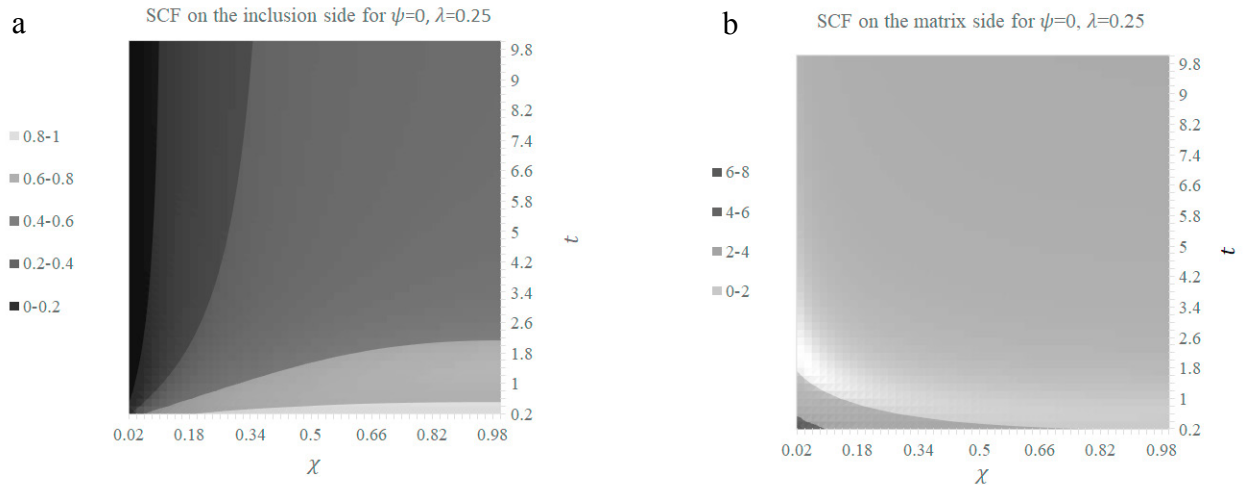

Fig. 10. Contour plot of the stress concentration factor on the inclusion side (a) and on the matrix side (b) for inclusion orientation angle $\psi = 0$, and porosity density $\lambda = 0.25$.

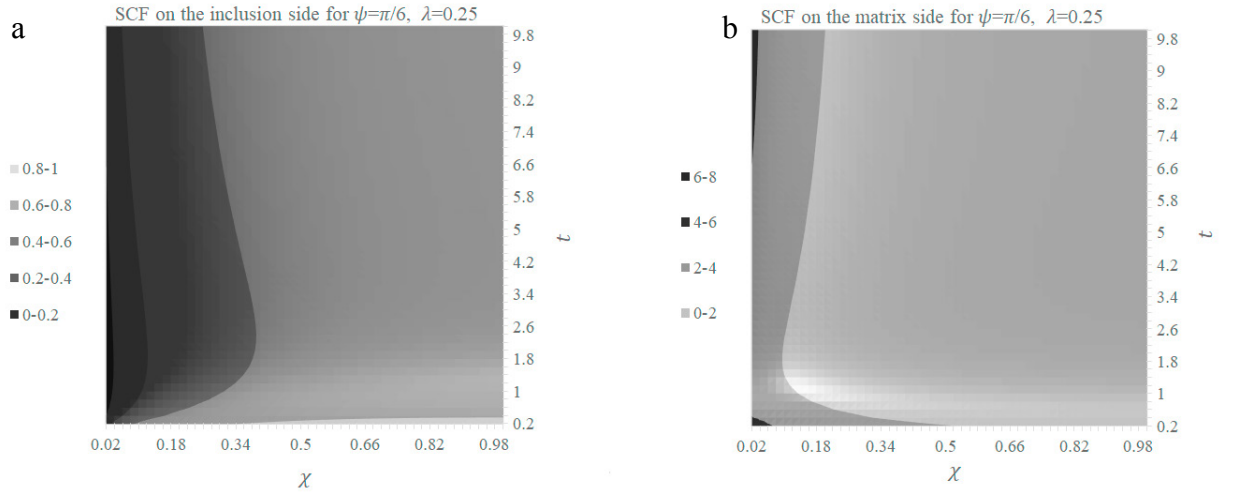

Fig. 11. Contour plot of the stress concentration factor on the inclusion side (a) and on the matrix side (b) for inclusion orientation angle $\psi = \pi/6$, and porosity density $\lambda = 0.25$.

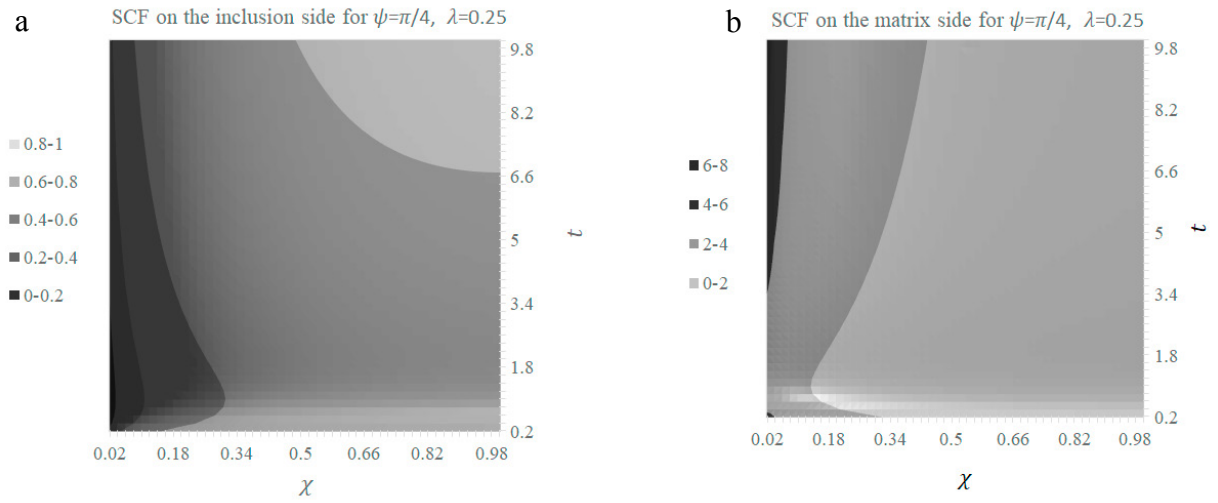

Fig. 12. Contour plot of the stress concentration factor on the inclusion side (a) and on the matrix side (b) for inclusion orientation angle $\psi = \pi/4$, and porosity density $\lambda = 0.25$.

4. Conclusions

In this paper, a multiscale approach for the stress analysis of defects clusters in an elastic matrix is proposed. The defects are assimilated to elliptical voids and the cluster is modeled as a porous elastic inclusion, whose elastic properties are weakened by the presence of the voids.
Firstly, the elastic properties of the inclusion have been calculated following the approach proposed by Weng (1984) and further developed by Tandon and Weng (1984, 1986), and by Zhao and Weng (1990). The approach, though approximated, allows to obtain simple explicit expressions for the effective Young's modulus and Poisson's ratio of an elastic, isotropic, infinite plate in plain strain, containing randomly distributed and randomly oriented elliptical pores. The effective elastic moduli, which depend only on the porosity density λ, the voids' aspect ratio χ, and the elastic moduli of the plate material, have been validated via a FE analysis.
Next, an equivalent elliptical inclusion with the calculated effective elastic properties and embedded in an infinite elastic plate under uniform uniaxial tension has been considered, as a simplified mechanical model of a defects cluster. To analyze the non-homogeneous stress field of the elliptical weakened inclusion in the matrix, the closed-form solution of Eshelby's problem proposed by Jin et al. (2014) has been implemented in MATLAB®, to calculate the stress peaks (SCFs) at the interface between the inclusion and the matrix. The dependence of the SCFs on the various microstructure parameters,

- porosity density λ,
- voids aspect ratio χ,
- inclusion aspect ratio *t*,
- inclusion orientation ψ,

is illustrated in Fig- 7-12. As expected, higher porosity densities correspond to higher SCFs, for any defects and inclusion shape. At a fixed porosity density, we have found that higher stress concentrations (>4) occur for voids and inclusion approaching a crack shape.

References

Costa, N., Machado, N., Silva, F., 2010. A new method for prediction of nodular cast iron fatigue limit, Internal Journal of Fatigue 32 (7), 988-995.

Cova M., Livieri P., Rizzoni R., Tovo R., 2017. A preliminary investigation of strength models for degenerate graphite clusters in grey cast iron. Procedia Structural Integrity 7, 446–452.

Eshelby, J.D., 1957. The determination of the elastic field of an ellipsoidal inclusion and related problems. In: Proceedings of the Royal Society A: Mathematical, Physical and Engineering Sciences, 241, pp. 376–396.

Eshelby, J.D., 1959. The elastic field outside an ellipsoidal inclusion. In: Proceedings of the Royal Society A: Mathematical, Physical and Engineering Sciences, 252, pp. 561–569.

Eshelby, J.D. 1961. Elastic inclusions and inhomogeneities. In N. Sneddon & R. Hill (Eds.), *Progress in Solid Mechanics*, vol. 2: 89–140. Amsterdam: North-Holland.

Feng X., Li J., Yu S., 2003. A simple method for calculating interaction of numerous microcracks and its applications, International Journal of Solids and Structures 40 (2), 447-464.

Hill, R., 1963. Elastic properties of reinforced solids: some theoretical principles, Journal of the Mechanics and Physics of Solids 11, 357-372.

Hütter, G., Zybell, L., Kuna, M., 2015. Micromechanisms of fracture in nodular cast iron: From experimental findings towards modeling strategies -A review. Engineering Fracture Mechanics 144, 118–141.

Jin X., Wang Z., Zhou Q., Keer L.M., Wang Q., 2014. On the solution of an elliptical inhomogeneity in plane elasticity by the equivalent inclusion method, Journal of Elasticity 114, 1-18.

Mottitschka, T., Pusch, G., Biermann, H., Zybell, L., Kuna, M., 2012. Influence of graphite spherical size on fatigue behaviour and fracture toughness of ductile cast iron EN-GJS-400-18LT. International Journal of Materials Research 103(1), 87–96.

Mori, T., Tanaka, K., 1973. Average stress in the matrix and average elastic energy of materials with misfitting inclusions, Acta Metallurgica 21, 571-574.

Rausch, T., Beiss, P., Broeckmann, C., Lindlohr, S., Weber, R., 2010. Application of quantitative image analysis of graphite structures for the fatigue strength estimation of cast iron materials. Procedia Engineering 2(1), 1283–1290.

Shen L., Yi S., 2001. An effective inclusion model for effective moduli of heterogeneous materials with ellipsoidal inhomogeneities. International Journal of Solids and Structures 38, 5789-5805.

Tandon G.P., Weng G.J., 1984. The effect of aspect ratio of inclusions on the elastic properties of unidirectionally aligned composites, Polymer Composite 5(4), 327-333.

Tandon G.P., Weng G.J., 1986. Average stress in the matrix and effective moduli of randomly oriented composite, Composite Science and Technology 27, 111-132.

Weng G.J., 1984. Some elastic properties of reinforced solids with special reference to isotropic ones containing spherical inclusions. International Journal of Engineering Science 22 (7), 845-856.

Zhao Y.H., Weng G.J., 1990. Effective elastic moduli of ribbon-reinforced composites, Transactions of the ASME 57, 158-167.

Zou W., 2011. Limitation of average Eshelby tensor and its application in analysis of ellipse approximation, Acta Mechanica Solida Sinica 24 (2), 176-184.

Zou W., He Q., Huang M., Zheng Q., 2010. Eshelby's problem of non-elliptical inclusions, Journal of the Mechanics and Physics of Solids 58, 346-372.